

A NUMERICAL STUDY ON THE DYNAMIC BEHAVIOR OF A THIN LIQUID FILM SUBJECT TO A VERTICAL OSCILLATION

María D. Giavedoni
*Instituto de Desarrollo Tecnológico para la Industria Química.
Universidad Nacional del Litoral-CONICET
Güemes 3450, Santa Fe, ARGENTINA*

ABSTRACT

In this work we investigate numerically the conditions for the onset of a two-dimensional wave motion on the free surface of a horizontal thin liquid layer subject to a vertical periodic acceleration of very small amplitude and very high frequency.

RESUMEN

En este trabajo investigamos numéricamente las condiciones para el desarrollo de un movimiento ondulatorio bidimensional en la superficie de una película líquida horizontal sometida a una aceleración periódica de muy pequeña amplitud y muy alta frecuencia.

INTRODUCTION

The stability of a liquid-air interface is a phenomenon primarily related to the atomization of liquids - an important method to produce a large transfer area between a gas and a liquid. In chemical engineering, liquid atomizers are employed in the execution of mass-transfer operations in which a small average drop size is required. Because the drop size is proportional to the inverse of the excitation frequency, it is possible to produce very small drops by means of ultrasonic atomization.

Faraday [1] was the first to notice that the free surface of a liquid becomes wavy when a vertical oscillation with a given frequency and amplitude is imposed to the container. He also reported that the frequency of the surface waves was one half the frequency of the forcing oscillation. Benjamin and Ursell [2] explained this subharmonic excitation of the surface waves analyzing the irrotational motion of an ideal fluid when the amplitude of the imposed oscillation is infinitesimally small. From their results they concluded that the system is always unstable under an imposed oscillation with a frequency equal to twice the natural frequency of the system considered, even if the force amplitude is very small. This unrealistic result is a consequence of the ideal behavior imposed to the liquid and of the elimination of nonlinear terms in the mathematical formulation.

Ockendon and Ockendon [3] extended the analysis of Benjamin and Ursell [2] to small but finite amplitudes and included nonlinear effects, and Miles [4] incorporated linear damping attributable to viscous effects. A number of experimental and theoretical studies have been carried out to study the formation of regular patterns in system with large aspect ratio. Gu et al., [5] studied 3-D nonlinear waves under vertical oscillations in the special case when only one spatial mode is strongly excited, and Virnig et al. [6] studied this problem experimentally; Milner [7], analyzed the influence of nonlinear interactions between different waves on the symmetry of regular patterns and Miles [8] extended this last work. All these works deal with the equation of motion of an incompressible inviscid fluid, in which linear or nonlinear damping terms for the amplitude are derived or evaluated.

The objective of this work is to study numerically the dynamic behavior of a horizontal liquid layer subject to ultrasonic vibrations. As a first step in the study of a three-dimensional problem, attention is restricted to the stability of thin liquid films respect to two-dimensional perturbations. This restriction is supported by experimental results [9] that show that the waves are two-dimensional at least when the instability is incipient.

The numerical technique here employed is based on the finite element method combined with a suitable parameterization of the free surface. This technique was formerly developed by Ruschak [10] and improved by Saito and Scriven [11] and Kistler and Scriven [12] for simulating steady viscous free surface flows. Keshgi and Scriven [13] studied steady viscous free surface flow problems combining this technique with the methodology proposed by Gresho et al. [14] for transient flows.

The numerical results presented in this work show the evolution of a thin liquid film subject to vertical oscillations for different values of the dimensionless numbers that characterize the system. Initially, the liquid is supposed to be motionless and the free surface adopts a sinusoidal shape. We show the existence of a critical amplitude of the imposed oscillation, for a fixed forcing frequency, beyond which a wavy motion of the free surface arises.

MATHEMATICAL FORMULATION

A horizontal layer of an incompressible viscous liquid is subject to an oscillatory vertical acceleration $a_0 \cos(\omega t)$ where a_0 is the amplitude and ω is the frequency of the imposed force. The air above the liquid is regarded as inviscid.

The liquid layer is extended on the horizontal plane (x, y) and its equilibrium height measured along the y -coordinate is h_0 . Figure 1 shows the coordinate system adopted and the imposed boundary conditions. u and v are the x - and y - components of the velocity vector, respectively; we suppose that the possible wave motion can be described as a function of one spatial coordinate (x) and time.

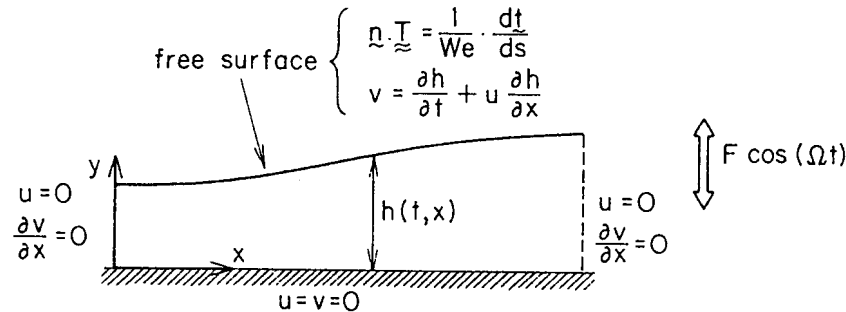


Figure 1: Schematic representation of the flow domain, boundary conditions and coordinate system adopted

We impose an initially sinusoidal perturbation of amplitude ϵ and wavenumber α , and we follow the temporal evolution of this disturbance. Fluid motion is governed by the physical laws of conservation of momentum and mass. These equations are made dimensionless by means of the following scales: h_0 (the mean film thickness) for lengths and $\sqrt{g/h_0}$ for time; g is the gravitational acceleration. Thus, the equations expressing conservation of momentum and mass are

$$\frac{\partial \mathbf{v}}{\partial t} + \mathbf{v} \cdot \nabla \mathbf{v} = -\nabla p + \frac{1}{Re} \nabla \cdot \boldsymbol{\tau} - (1 - F \cos \Omega t) \mathbf{g} \quad (1)$$

$$\nabla \cdot \mathbf{v} = 0 \quad (2)$$

In all cases considered here, the viscous stress τ is that of an incompressible Newtonian fluid: $\tau = \nabla v + (\nabla v)^T$. The unit vector g is in the direction of the gravitational force. $\Omega = \frac{\rho \sqrt{g h^3}}{\mu}$ is the Reynolds number, $\Omega = \frac{\omega^2 h^3}{\nu}$ enters the formulation as a component of the gravitational field and it gives the ratio between the external imposed forces and the gravitational forces, and $\Omega = \frac{\omega h^3}{\nu}$. The liquid density is ρ and its viscosity is μ .

The Navier-Stokes equation requires a boundary condition on every portion of the flow domain. At solid boundaries the non-slip condition is imposed,

$$v = 0 \quad (3)$$

At the gas-liquid interface continuity of stresses is expressed as

$$n \cdot T = \frac{1}{\sigma} t \quad (4)$$

where n is the outward pointing unit normal to the free surface and t is the unit tangent to the free surface, $We = \frac{\rho U^2 h}{\sigma}$ is the Weber number.

In the presence of a free surface, the flow domain is an unknown function of time but the interface is a material surface because mass is not transferred through it. The expression of mass conservation is the kinematic condition, that for a two-dimensional flow in the plane (x, y) is

$$v = \frac{\partial h}{\partial t} + u \frac{\partial h}{\partial x} \quad (5)$$

where $h = h(x, t)$, a function of time and one spatial coordinate only, is the local thickness of the liquid film.

NUMERICAL TECHNIQUE

The spatial discretization of the governing equations is based on the Galerkin/finite element method and a suitable parameterization of the free surface [12]. The flow domain is partitioned into a set of quadrilateral elements; each element is limited by two straight sides, formed by fixed spines of constant x , and by two curve sides which reflect the shape of the free surface. These elements are mapped isoparametrically on the unit square with coordinates (ξ, η) , $0 \leq \xi, \eta \leq 1$, by means of the nine biquadratic basis functions used in the expansions representing the components of the velocity,

$$x(\xi, \eta) = \sum_j x^j \Phi^j(\xi, \eta) \quad (6)$$

$$y(\xi, \eta) = \sum_j y^j(t) \Phi^j(\xi, \eta) \quad (7)$$

where $(x^j, y^j(t))$ are the coordinates of the nodes. The mesh adopted in this work has spines parallel to the y -axis, therefore, the coordinates of the nodes located along a given spine have fixed values of x , a fact taken into account when building the Jacobian matrix in the numerical code ([15]). In the computational domain the free surface is a line of constant η , ($\eta = 1$) and it is approximated by the one-dimensional specialization of the biquadratic basis functions,

$$y_{FS} = \sum_{j=1}^3 h^j(t) \Phi^j(\xi, \eta = 1) \quad (8)$$

In equation (8), $h^j(t)$ are the coefficients of the gas-liquid interface parameterization; they represent the distance along a given spine from the x -axis to the free surface.

Mixed interpolation is used to approximate velocity and pressure fields. Thus we have,

$$v(x, t) = \sum_j v^j(t) \Phi^j(\xi, \eta) \quad (9)$$

$$p(x, t) = \sum_k p^k(t) \Psi^k(\xi, \eta) \quad (10)$$

where $v^j(t)$ and $p^k(t)$ are unknown time dependent nodal values and $\Psi^k(\xi, \eta)$ are the four bilinear basis functions defined on the standard square.

The residuals of the weighted equations of the momentum, mass and kinematic condition yield a set of nonlinear ordinary differential equations. These residuals include the time derivatives of the velocity and free surface location coefficients, which are Eulerian time derivatives. The tessellation generated by the spine parameterization of the free surface constrains the nodes to move along a particular line in the space (a spine) in order to follow the deformation of the free surface and this fact must be taken into account in the evaluation of time derivatives ([13], [16]). Since any given node has fixed isoparametric coordinates, time derivatives can be thought of time derivatives at a fixed point in the (ξ, η) space:

$$\dot{v} = \frac{\partial v}{\partial t} + \dot{x} \cdot \nabla v \quad \dot{v} = \sum \frac{dv^j}{dt} \Phi^j(\xi, \eta) \quad (11)$$

In equation (11) \dot{x} is the velocity of a point with fixed isoparametric coordinates and it is evaluated from equations (6) and (7),

$$\dot{x} = \left(\frac{\partial x}{\partial h} \right) \left(\frac{dh}{dt} \right) \quad (12)$$

In order to transform the system of nonlinear ordinary equations into a set on nonlinear algebraic equations, \dot{v} and \dot{x} are approximated by finite-differences. We proceed as follows,

- A trapezoid-rule corrector is used to approximate \dot{v} and \dot{x} in the weighted residuals of both, the momentum equation and the kinematic condition.
- The set on nonlinear equations obtained is solved by means of one-step Newton's method ([14]).
- The second-order accurate Adams-Bashforth predictor is used to provide an accurate initial approximation for Newton's method and an estimate of time discretization error [13]. The discretization error is kept small in order to obtain a predicted initial approximation accurate enough so that the required convergence is reached in just one Newton iteration. Pressure coefficients are initialized with values corresponding to the previous time step.
- Following [17], the numerical scheme is started up with four backward-difference corrector steps while a forward-difference predictor is used and the size of the time step is kept constant. This procedure generates the information needed by the trapezoid-rule corrector and avoids the oscillations that certain initial conditions can introduce when this second order corrector is used.
- From the fifth time step on, the Adams-Bashforth predictor and the trapezoid-rule corrector are used. Beginning with the sixth time step, the size of the step is automatically adjusted according

to the tactics proposed by Gresho et al. [14]. This adjustment keeps the time discretization error within each step below a preset level.

We have evaluated two time steps. One, Δt_v , based on the norm of the velocity and the other, Δt_h , based on the norm of the free surface coefficients. Thus, at the beginning of time step $n+1$, we have

$$\Delta t_v^{n+1} = \Delta t^n \left(\frac{\kappa}{|\delta_v^n|} \right)^{1/3}, \quad \Delta t_h^{n+1} = \Delta t^n \left(\frac{\kappa}{|\delta_h^n|} \right)^{1/3} \quad (13)$$

where κ is the prescribed value of the norm of the error at time $n+1$ and it is selected to hold within bounds the total discretization error at each time step; $|\delta_v^n|$ is the norm of the local time truncation error, at time n , based on the velocity coefficients and evaluated according to [14] and, similarly, $|\delta_h^n|$ is the norm of the local time truncation error based on the norm of the free surface location coefficients. Following [18], we have chosen

$$\Delta t = \min(\Delta t_v, \Delta t_h) \quad (13)$$

in order to attain accuracy in the calculations. Details concerning the time step selection are discussed in [14].

FINITE ELEMENT SOLUTIONS.

As we have already mentioned in the introduction of this work, we are searching the conditions under which it is possible to produce a wave motion at the air-liquid interface of a thin liquid layer, when the dimensions of the system are large compared to the wavelength of the final pattern developed.

We have carried out computations in order to study the influence of the initial condition imposed to the free surface and the amplitude of the external acceleration.

1) Influence of the initial condition.

At $t = 0$ we impose the following sinusoidal perturbation on the free surface:

$$y_{fs}(x, 0) = 1 + \varepsilon \sin\left(\alpha x - \frac{\pi}{2}\right), \quad 0 \leq x \leq \frac{\pi}{\alpha}$$

Therefore, two parameters can be varied in order to study the influence of the initial perturbation: the amplitude ε and the wavenumber α . We fix ε in a value large enough compared to the final wave amplitude expected and vary α . The mesh is refined near the free surface in both tessellations. The dimensionless numbers that characterize the behavior of the system adopt the following values:

$$\begin{aligned} Re &= 98.99 \\ We^{-1} &= 7.14 \\ F &= 7251 \\ \Omega &= 1904 \end{aligned}$$

They result for the special case in which the amplitude (a_0) of the imposed acceleration is equal to $2 \times 10^{-6} m$ and its frequency (ω) is $3 \times 10^4 Hz$; $\mu = 10^{-3} Pa.s$, $\rho = 10^3 kg/m^3$ and $\sigma = 70 \times 10^{-3} N/m$.

Our numerical results (that are not illustrated here) show that the behavior of the system depends on the wavenumber of the initial excitation. In fact, for $\alpha \geq 5$, the amplitude of the disturbance monotonously decays until a final flat interface is achieved. Although results are not depicted here, the computations

performed predict the same behavior for larger values of the wavenumber. (Numerical evaluations have been carried out for $\alpha \leq 20$).

For $\alpha = 3$, the amplitude of the initial disturbance decays but not in a monotonous way. In fact, when $t \approx 2.5$ a small increase in the maximum film thickness is observed. Nevertheless, our results suggest that a motionless horizontal film should be expected at larger values of time.

For $\alpha = 1$ and $\alpha = 2$, the amplitude of the initial perturbation increases. In order to determine if these results are a consequence of the external vibration imposed, we have followed the evolution of the same initially sinusoidal free surface when gravity is the only external force acting on the system, i.e. when $Re = 98.99$, $We^{-1} = 7.14$ and $F = 0$. The numerical results obtained in this case (that are not depicted here) show that the amplitude of the initial disturbance imposed to the gas-liquid interface decays for any value of α ; therefore, the dynamic behavior of the system is different whether or not a vertical periodical acceleration is imposed to the liquid. When $\alpha \leq 2$, the evolution of the free surface profile shows that the wavenumber of the initial perturbation remains constant throughout the computations; from very simple calculations it is easy to verify that the frequency of the growing perturbation is much smaller than the frequency of the external force. Since we are interested in the description of surface waves coming from a parametric excitation, i.e. waves of high frequency, we have not followed these computations for larger values of time in order to determine if a time-periodic or an unstable solution results for these values of the wavenumber. Instead we have studied the influence of the amplitude of the vertical acceleration on the evolution of an initially small disturbance ($\alpha = 20$).

2) Influence of a_0 .

The wavenumber of the initial perturbation imposed to the free surface is fixed in 20 and its amplitude, ε , is equal to 0.01. Liquid density (ρ) is equal to 10^3 kg/m^3 , liquid viscosity (μ) is equal to 10^{-3} Pa.s , the surface tension of the gas-liquid interface (σ) is fixed in $70 \times 10^{-3} \text{ N/m}$, and the thickness of the levelled film is 10^{-3} m . All these parameters are kept constant in these computations. Changes in a_0 imply changes in F ; if a_0 increases so does F . To increase F under the aforementioned conditions, implies to increase the strength of the imposed force respect to viscous, capillary and gravity forces.

The time evolution of the initial disturbance is shown in Figure 2. According to these results, there exists a critical value of F beyond which a wave motion arises.

When $F = 7251$ ($a_0 = 2 \times 10^{-6} \text{ m}$), the initial perturbation rapidly decays and a quiescent flat film is finally obtained. The time-evolution of the velocity field for $F = 7251$, which is not depicted here, shows that only near the free surface the motion of the fluid is important and that the fluid remains almost motionless at a very short distance from it. Although surface velocities are quite large for $t \rightarrow 0$, they decay fast as the film is being levelled.

Similar results are obtained for $F = 14,502$ ($a_0 = 4 \times 10^{-6} \text{ m}$). When $F = 21,753$ ($a_0 = 6 \times 10^{-6} \text{ m}$) the amplitude of the initially imposed disturbance decays but the evolution of the film thickness does not present a regular pattern at the beginning of the process. In this case, when a time-periodic state is finally developed, the result is that the free surface adopts a wavy shape completely different to the initially imposed one. The amplitude of the standing wave is smaller than the amplitude of the initial perturbation and from simple calculations it is easy to verify that its circular frequency is about $95,000 \text{ rad/s}$, a value very near to half of the frequency of the imposed acceleration.

If F is further increased ($F = 29,004$ ($a_0 = 8 \times 10^{-6} \text{ m}$)) the system experiments a very short transient during which the maximum film thickness increases and the initial sinusoidal shape imposed on the free surface is also modified as it is illustrated in Figure 2. After this initial period, the disturbance evolves until a time-periodic state is established. In this case the standing wave has an amplitude greater than that of the initial perturbation and its frequency is, again, approximately half of the frequency of the imposed acceleration.

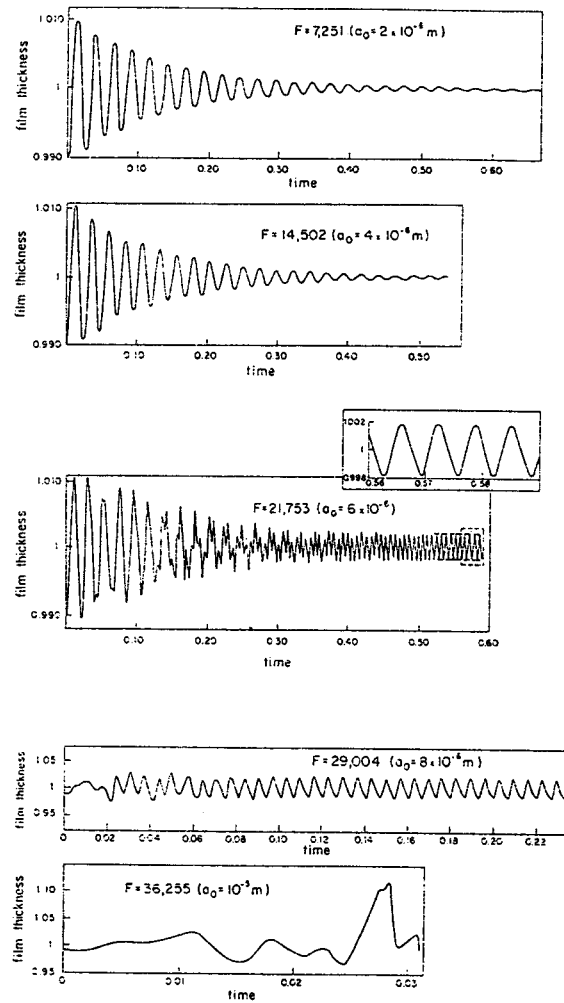


Figure 2: Prediction of the time-evolution of the film thickness at $x = 0$, for different values of the amplitude of the imposed acceleration. $Re = 98.99$, $We^{-1} = 7.14$ and $\Omega = 1904$.

Figure 3 illustrates the features of the time-periodic state developed in this case. Sequences of free surface shapes depicted here show that more than one mode is excited in the time-periodic state, a result that agrees with theoretical results previously reported ([5], [7], [8]). In this figure E_4 is the

dimensionless kinetic energy, $E_k/E_s(0)$ is the ratio between the surface energy at time t and the surface energy at the beginning of the computations. They are evaluated with the following expressions

$$E_k(t) = \frac{E_k^*(t)}{\rho(g h_0) h_0^2} = \frac{1}{2} \int_{x=0}^{\pi/a} \int_{y=0}^{h(x)} (u^2 + v^2) dx dy \quad (15)$$

$$E_s(t) = \frac{E_s^*(t)}{\sigma h_0} = \int_0^{s'} ds \quad (16)$$

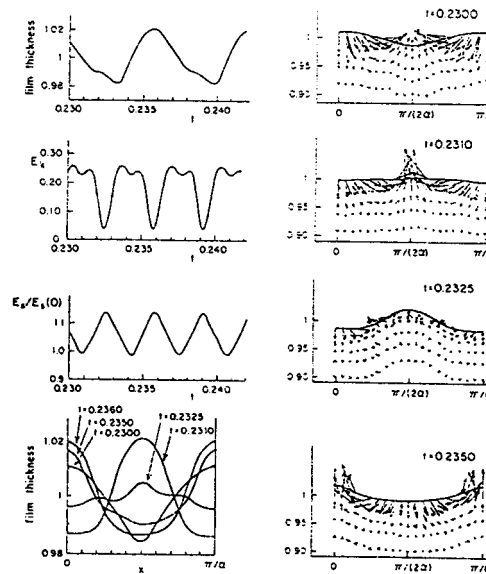


Figure 3: Relevant features of the time-periodic state developed for $Re = 98.99$, $We^{-1} = 7.14$, $\Omega = 1904$ and $F = 29,004$.

When $F = 36,255$ ($a_0 = 10^{-5} m$), the numerical calculations carried out in this work point out that a time-periodic state is not attained in this case (see Figure 2). In fact, the sequence of free surface shapes obtained (that are not illustrated here) shows that the initial perturbation imposed to the free surface evolves into a number of irregular waves of high spatial frequency; the amplitude of some of these waves grows without bounds and, finally, the film rupture is produced.

A schematic representation of the behavior of the liquid film under study is portrayed in Figure 4. According to our numerical results, there exists a critical value of F (F_c) at which a time-periodic wavy state bifurcates from the flat steady-state. When $F < F_c$, disturbances of small amplitude decay while if

$F > F_c$, solutions approach a time-periodic state with amplitudes depending on the amplitude of the external force. The frequency of the dominant standing wave is about one half the frequency of the imposed acceleration and secondary waves are also detected. However, if F is further increased, the amplitude of the disturbance grows until the rupture of the liquid film is produced.

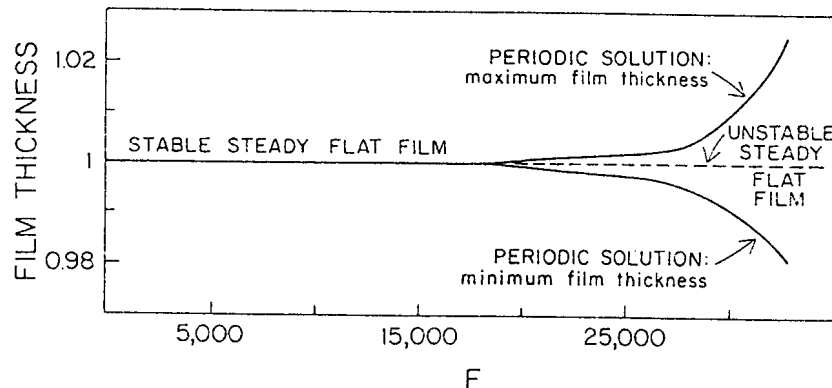


Figure 4 Domain representation of the time-periodic states predicted by the finite element solutions for $Re = 98.99$, $We^{-1} = 7.14$ and $\Omega = 1904$.

CONCLUSION

The numerical results reported in this work give a good qualitative description of the behavior of a thin liquid film subject to a vertical oscillation. The main assumption we have made is to suppose that waves of small amplitudes are, at least when the instability is incipient, two-dimensional, a hypothesis supported by experimental evidences. This is the first time, up to our knowledge, that a numerical solution of the complete set of equations and boundary conditions is reported.

In agreement with experimental results, our results predict the existence of a critical value in the amplitude of the imposed acceleration beyond which the motion of the liquid arises. They also show that time-periodic solutions are possible in a range of values of this parameter. In fact, if the amplitude is high enough, the system becomes unstable without passing through a time-periodic state.

REFERENCES

- 1 Faraday, M. "On the forms and states assumed by fluids in contact with vibrating elastic surfaces", *Phil. Trans. R. Soc. London* 1831, **121**, 319.
- 2 Benjamin, T.B. and F. Ursell, "The stability of the plane free surface of a liquid in a vertical periodic motion", *Proc. R. Soc., Ser A*, 1954, **225**, 505.
- 3 Ockendon, T.B. and H. Ockendon, "Resonant surface waves", *J. Fluid Mech.* 1973, **59**, part 2, 397
- 4 Miles, J.W., "Nonlinear Faraday resonance", *J. Fluid Mech.* 1984, **146**, 285.
- 5 Gu, X.M., P.R. Sethna and A. Narain, "On three-dimensional nonlinear subharmonic resonant surface waves in a fluid. Part I - Theory", *ASME J. Appl. Mech.* 1988, **55**, 213.

- 6 Virmig, J.C., A.S. Berman, and P.R. Sethna, "On three-dimensional nonlinear subharmonic resonant surface waves in a fluid. Part II - Experiment", *ASME J. Appl. Mech.* 1988, **55**, 213.
- 7 Milner, S.T, "Square patterns and secondary instabilities in driven capillary waves", *J. Fluid Mech.* 1991, **225**, 81.
- 8 Miles, J.W, "On Faraday waves", *J. Fluid Mech.* 1993, **248**, 671.
- 9 Hasegawa, E., T Umehara and M. Atsumi, "The critical condition for the onset of waves on the free surface of a horizontal liquid layer under a vertical oscillation", *Bull. JSME* 1984, **27**, 1625.
- 10 Ruschak, K.J., "A method for incorporating free boundaries with surface tension in finite element fluid flow simulators", *Int. J. Num. Meth. Engng.* 1980, **15**, 639.
- 11 Saito, H. and L.E. Scriven, "Study of coating flow by the finite element method", *J. Comp. Phys.* 1981, **42**, 53.
- 12 Kistler, S.F. and L.E. Scriven, "Coating flow computations". Computational analysis of polymer processing. Pearson, J.R.A. and Richardson, S.M., Eds.; Applied Science Publishers: London 1983, Ch 8, pp 243-299.
- 13 Kheshgi, H.S. and L.E. Scriven, "Penalty finite element analysis of unsteady free surface flows", *Finite elements in fluids*, vol. 5. Gallaher, R.H.; Oden, J.T.; Zienkiewicz, O.C.; Kawai, T. and Kawahara, M., Eds; Wiley: New York 1984, p. 393.
- 14 Gresho, P.M., R.L Lee and R.L Sani, "On the time-dependent solution of the incompressible Navier-Stokes equations in two and three dimensions", *Recent advances in numerical methods in fluids*, vol. 1. Taylor, C. and Morgan, R, Eds; Pineridge Press, Ltd.: Swansea, U.K. 1979.
- 15 Patzek, T.W., R.E. Benner Jr., O.A. Basaran, and L.E. Scriven, "Nonlinear oscillations of inviscid free drops", *J. Comp. Phys.* 1991, **97**, 289
- 16 Keunings, R., "An algorithm for the simulation of transient viscoelastic flows with free surfaces", *J. Comp. Phys.* 1986, **62**, 199.
- 17 Luskin, M. and R Rannacher, "On the smoothing property of the Crank Nicholson scheme", *Applicable Analysis* 1982, **14**, 117
- 18 Wambersie, O. and M.J. Crochet, "Transient finite element method for calculating steady state three-dimensional free surfaces", *Int. J. Num. Meth. Fluids* 1992, **14**, 343-360.